Implications of IM selection for seismic Loss Assessment of 3D Buildings

Mohsen Kohrangi,[1] **M.EERI Dimitrios Vamvatsikos,**[2] **M.EERI**

and Paolo Bazzurro,[3] **M.EERI**

Present building-specific loss assessment state-of-art involves the convolution of seismic hazard and building seismic demands. The latter is conditioned on spectral acceleration, $Sa(T_1)$, at the building first mode as the ground motion intensity measure (IM) and is typically estimated by carrying out nonlinear dynamic analyses on a 2D model. By new proposals on the use of improved IMs that can introduce higher fidelity, the accuracy in loss estimation becomes an open question. In reply, we offer a uniform basis for comparing the loss estimates for a set of eight different scalar and vector IMs whose hazard can be predicted with existing GMPEs. Despite all eight being legitimate IMs, and the consistent use of Conditional Spectrum record selection, we find large differences in the estimated loss hazard. This points to the large uncertainty still lingering when connecting hazard to loss. Among the IMs considered here, the vector IMs and at least a scalar average of spectral accelerations showed a remarkable stability in their predictions for the 3D buildings, pointing to a potential for reliable applications.

INTRODUCTION

In active seismic regions, earthquakes might happen during the life cycle of the building causing life, monetary and downtime losses. In recent years methodologies have emerged to

[1] Istituto Universitario di Studi Superiori, IUSS, Pavia, Italy: email: mohsen.kohrangi@umeschool.it

[2] Lecturer, School of Civil Engineering, National Technical University of Athens, Athens, Greece.

[3] Professor, Istituto Universitario di Studi Superiori, IUSS, Pavia, Italy.

quantify these losses as the basis to make informed decisions about earthquake risk mitigation. In general, these methods could be divided into two main categories, namely regional and building-specific loss estimation approaches. This study is mainly concentrated on the latter, although the results of such building-specific studies are also useful to regional loss estimation.

The common approach to building-specific loss estimation is the integration of the hazard of the site with the building demands estimated via a nonlinear response history analysis typically of a 2D model of the building. The severity of the ground motion is often measured by $Sa(T_1)$, which is the spectral acceleration at the first modal period of vibration of the structure. It is well known that a good intensity measure (IM) for this scope should be efficient, sufficient and practical. An efficient IM is a good predictor of the structural response, namely it provides low dispersion in the distribution of the engineering demand parameters (EDPs) selected to gauge the response given the IM, thus requiring only a low number of records in order to reach a stable estimate of the EDP distribution. An IM is sufficient when the distribution of building EDPs conditioned on this IM is independent of other ground motion properties such as magnitude of the causative earthquake, distance from site to rupture, etc. Finally, practicality refers to the availability of such an IM for hazard computations, or in other words, to the existence of Ground Motion Prediction Equations (GMPEs) for that IM.

The accuracy of this common approach, however, is questionable. Firstly, during the recent years, several IMs have been shown to outperform $Sa(T_1)$ for EDP prediction. Secondly, recent studies have shown that a reliable (efficient and sufficient) characterization of the EDP distribution given the IM is not a straightforward task especially for complex 3D structural models under multi-directional excitations (Lucchini et al., 2011; Faggella et al., 2013), for tall buildings (Shome and Cornell, 1999) or for buildings located at sites close to active faults where near-source type ground motions can be expected (Luco, 2002; Baker and Cornell, 2008). Thirdly, there are building components that are sensitive to more than one EDPs, such as infill masonry walls whose collapse damage state is sensitive to in-plane peak inter-story drift (IDR) and out-of-plane peak floor acceleration (PFA) jointly and

simultaneously (Barrera, 2015 and Mosalam and Günay, 2015). An IM that is well correlated with the building response in the two main horizontal directions would decrease the uncertainty in the damage assessment of such components.

The complexities mentioned above suggest the necessity of exploring the availability of efficient, sufficient and practical IMs that reduce the uncertainty and bias in estimated losses, while maintaining the applicability and simplicity of the assessment procedure. In addition, most of the efforts in recent investigations on loss estimation were based on 2D structural models and scalar IMs (Porter et al., 2001; Porter et al., 2002; Aslani, 2005; Goulet et al., 2007; Mitrani-Reiser, 2007; Bradley et al., 2009b; Ramirez, 2009; Jayaram et al., 2012). In the realm of more elaborate scalar IMs, Kazantzi and Vamvatsikos (2015) showed that an average spectral acceleration, defined as the average of logarithmic values of spectral accelerations computed at different periods, is capable of capturing within an acceptable level of dispersion the response in terms of IDR and PFA all along the building height. Jayaram et al. (2012) went beyond scalar IMs and used a vector of spectral accelerations at multiple periods in response prediction for development of vulnerability functions for tall buildings. Along similar lines, Modica and Stafford (2014) developed vector fragility surfaces that use two correlated IMs for reinforced concrete (RC) frames in Europe. Beyond 2D models, Kohrangi et al. (2015c) observed that for buildings modeled in 3D, providing a direction insensitive IM, such as the geometric mean of Sa(T_1), into two orthogonal components of the excitation (i.e. IMX and IMY in a two component vector) helps improving the accuracy of the response estimates. However, the advantages potentially brought by such advanced IMs (either scalar or vector) have not been carried forward to be tested in the assessment of loss.

Following the work of Kohrangi et al. (2015b) that carried out hazard estimation for different spectral acceleration-based scalar and vector IMs, and Kohrangi et al. (2015c) who studied the effect of such IMs on the estimation of structural response, we now extend this investigation to the estimation of losses. The aim is to understand the influence of the choice of the IM, which represents the severity of the ground motion and, therefore, the link to the hazard, on the loss estimates for three existing reinforced concrete buildings located at a seismically active site.

SEISMIC LOSS ASSESSMENT FRAMEWORK

Performance Based Earthquake Engineering (PBEE) has emerged to provide tools and develop methodologies for estimating the losses induced by probable future earthquakes. In the last decade, the Cornell-Krawinkler framing equation, adopted by the Pacific Earthquake Engineering Research Centre (PEER), has become the mainstream approach to PBEE. It comprises a four-step methodology that combines: i) Hazard Analysis, ii) Demand Analysis, iii) Damage Analysis, and, iv) Loss calculations, in a full probabilistic approach that takes into account different sources of uncertainty for the estimation of losses due to future seismic events. This procedure is summarized in Equation (1):

$$\lambda(DV) = \iiint \mathrm{G}(DV \mid DM) \cdot \left|\mathrm{dG}(DM \mid EDP)\right| \cdot \left|\mathrm{dG}(EDP \mid IM)\right| \cdot \left|\mathrm{d}\lambda(IM)\right| \qquad \textbf{Dis}$$

In this equation, IM is the Intensity Measure that gauges the level of ground motion severity and that is also used for structural response estimation. Probabilistic Seismic Hazard Analysis (PSHA) provides the Mean Annual Rate (MAR) of exceeding any given level of seismic intensity, $\lambda(IM)$. Theoretically, this IM can be any ground motion property in scalar or vector format. Whatever it is, it should be an appropriate representation of the ground motion, on one hand, and a proper structural response predictor, on the other hand. As mentioned earlier, EDPs can be the Peak Floor Acceleration (PFA), the peak Inter Story Drift ratio (IDR), as adopted by FEMA P-58 (2012), or whatever other structural response measure, perhaps indicative of local damage such as plastic rotations or curvature, that the engineer deems necessary. DM is the damage measure (typically discretized in a number of damage states) and DV represents one or more Decision Variables (or performance measures) that are meant to support decision-making by stakeholders. These variables are commonly defined as monetary losses, downtime and casualties. G(·) is the complementary cumulative distribution function (CCDF), and $\lambda(\cdot)$ is the function of the mean annual rate of exceeding values of its argument, here the IM. These quantities are blended in Equation (1), which integrates elements of hazard analysis, structural response analysis, damage evaluation and loss assessment to assist in the decision-making process (Mitrani-Reiser, 2007). The

most practical approach for numerical computations of Equation (1) is performing the integration via Monte Carlo simulation, which is also the method used in this study.

The connection of IM and EDP requires careful structural modeling and nonlinear analysis for the estimation of G(*EDP*|*IM*) distribution. This could be obtained by Incremental Dynamic Analysis (IDA) (Vamvatsikos and Cornell, 2002), or by means of cloud or multiple stripe analysis (Baker, 2007; Jalayer and Cornell, 2009). In order to associate the derived EDP levels with structural damage, fragility functions (or curves) for specific Damage States (DS) of specific components (e.g., columns, partitions, etc.) are employed (see Kennedy and Ravindra, 1984 for one of the earliest studies and Porter et al. (2007) for one of the recent ones). For each component and damage state, a corresponding cost function is used for cost analysis of repair actions and losses. By integrating the losses of all components in the building over their entire range of response and potential states of damage given the IM, one can generate the so-called vulnerability (or, somewhat improperly, damage) functions that provide a complete probabilistic characterization of seismic loss of the entire building at each IM level. FEMA P-58 (2012), as a result of the research efforts at US Federal Emergency Management Agency (FEMA), currently provides the most recent guidelines that form the state-of-the-art in the probabilistic estimation of the seismic loss for buildings. These guidelines along with the component-based fragility curve database and the cost functions and the companion software (called PACT) provide the necessary tools for carrying out the full procedure explained above. To this end, the user needs to group the structural and non-structural components and building contents into sub-groups that are expected to have the same behavior and damageability, and that are sensitive to the same EDP. Such structural components are defined based on the same fragility curves that are functions of the same EDP. These component-based fragility functions are based mainly on either IDR or PFA at the story where the components are located. In each response analysis, besides monitoring damage/losses at the component level, maximum residual inter story drift ratio (MrIDR) of the global structure is also monitored to ascertain whether the building can be repaired, whether it is collapsed or whether is still standing but should be demolished (and replaced). Commonly, an empirical fragility curve is used to define the probability of non-reparability (i.e., demolition) given the MrIDR value (Ramirez and Miranda, 2009).

For each ground motion record, once the structural response is estimated in the two main orthogonal directions in terms of different EDPs at each story, the damage state of each component is simulated through the fragility functions (or surfaces); consequently, using the corresponding repair costs distribution of each damage state and each building component, the repair costs of the damaged components for all considered limit states are computed. This exercise is done a number of times for each ground motion and repeated for all ground motions at each IM level. Based on FEMA P-58 (2012), the fragility curves (or surfaces) are usually assumed to be log-normally distributed and the repair functions are assumed to be normally distributed.

The loss estimates are the output of custom software that performs this comprehensive Monte Carlo simulation to estimate the vulnerability for both scalar and vector IMs while explicitly accounting for the uncertainties in all the different aspects of the problem. It should be noted that, for any given ground motion and realization of the component-by-component repair cost, the overall integrity of the building is also simulated given the value of MrIDR. More precisely, a simulation is performed on whether the building has collapsed and, if not, whether it is repairable. If the simulation indicates that the building is collapsed or non-repairable, then the loss for that simulation is equal to the total building replacement cost plus, in the latter case, the cost of demolition. The collapse definition is discussed in the subsequent sections. Note that for all the records at each IM level, the software tool provides the disaggregation of the expected repair cost for each component type (structural, non-structural, contents or specific components) or due to collapse and non-reparability (Mitrani-Reiser, 2007; Aslani, 2005). This detailed information is useful for understanding what parts of the structure are most vulnerable and potentially help guide appropriate retrofitting schemes.

SCALAR AND VECTOR IMs CONSIDERED IN THIS STUDY

In order to compare the uncertainty introduced to the losses estimated using Equation 1 from the response estimation based on different conditioning IMs, we considered the group of scalar and vector IMs listed in Table 1. The goal is to study the effectiveness in estimating the EDPs of the most natural predictors available to engineers, namely the elastic spectral

accelerations at different periods used singularly or jointly. We carried out this analysis for 3D models of buildings, as opposed to 2D models, as usually done. In Table 1 the names of all the IMs that are composed of spectral accelerations start with *Sa*. The first index, either *S* or *V*, defines whether the IM is a scalar or a vector. The second index is meant simply to distinguish each Sa-based IM from another. Note that, for historical reasons more than anything else, we also consider PGA as a predictor for the EDPs.

Table 1. IMs considered in the response estimation

INTENSITY MEASURE (IM) **	**ABBREVIATION***
SCALAR IMs	
Natural logarithm of arbitrary spectral acceleration at the first modal period $\ln\left[Sa_x(T_{1x})\right]$ or $\ln\left[Sa_y(T_{1y})\right]$.	Sa_{S1}
Natural logarithm of the geometric mean of spectral acceleration at the average period, $\ln\left[Sa_{g.m.}\left(\overline{T}=\left(T_{1x}+T_{1y}\right)/2\right)\right]$.	Sa_{S2}
$\ln\left[Sa_x\left(\alpha_1\cdot T_{1x}\right)\cdot Sa_x\left(T_{1x}\right)\cdot Sa_x\left(\alpha_u\cdot T_{1x}\right)\cdot Sa_y\left(\alpha_1\cdot T_{1y}\right)\cdot Sa_y\left(T_{1y}\right)\cdot Sa_y\left(\alpha_u\cdot T_{1y}\right)\right]$	Sa_{S3}
$\ln\left(\left[\prod_{i=1}^{n}\left(Sa_x\left(T_{xi}\right)\right)\right]^{1/n}\right)\cdot\ln\left(\left[\prod_{j=1}^{m}\left(Sa_y\left(T_{yj}\right)\right)\right]^{1/m}\right),\ \alpha_1\cdot T_1\le T_i\le\alpha_u\cdot T_1, m=n=10$ §	Sa_{S4}
Natural logarithm of the geometric mean of Peak Ground Acceleration, $ln[PGA_{g.m.}]$	PGA
VECTOR *IM*s	
$\ln\left\{Sa_x(T_{1x}),\frac{Sa_y(T_{1y})}{Sa_x(T_{1x})},\frac{Sa_x(1.5\cdot T_{1x})}{Sa_y(T_{1y})},\frac{Sa_y(1.5\cdot T_{1y})}{Sa_x(1.5\cdot T_{1x})}\right\}$	Sa_{V1}
$\ln\left\{Sa_{g.m.}(\overline{T}),\frac{Sa_{g.m.}(0.5\cdot\overline{T})}{Sa_{g.m.}(\overline{T})},\frac{Sa_{g.m.}(1.5\cdot\overline{T})}{Sa_{g.m.}(0.5\cdot\overline{T})}\right\}$	Sa_{V2}
$\ln\left\{\left[Sa_x\left(\alpha_1\cdot T_{1x}\right)\cdot Sa_x\left(T_{1x}\right)\cdot Sa_x\left(\alpha_u\cdot T_{1x}\right)\right]^{1/3},\left[Sa_y\left(\alpha_1\cdot T_{1y}\right)\cdot Sa_y\left(T_{1y}\right)\cdot Sa_y\left(\alpha_u\cdot T_{1y}\right)\right]^{1/3}\right\}$	Sa_{V3}
$\ln\left\{\left(\left[\prod_{i=1}^{n}\left(Sa_x\left(T_{xi}\right)\right)\right]^{1/n}\right),\left(\left[\prod_{j=1}^{m}\left(Sa_y\left(T_{yj}\right)\right)\right]^{1/m}\right)\right\},\ \alpha_1\cdot T_1\le T_i\le\alpha_u\cdot T_1, m=n=10$	Sa_{V4}

*All the IMs are based on natural logarithm transformation. The notation ln is removed from the abbreviations for brevity.
** α_1 is equal to 0.8, 0.2 and 0.2 for the 3-, 5- and 8-story, respectively. α_u is equal to 1.5 in all cases.
§ The periods are equally spaced.

More precisely, Sa_{S1} corresponds to the simple spectral acceleration at the first mode period of the structure in X or Y directions of the building. Sa_{V1} corresponds to a four-component vector IM that includes the first modal periods of the building in X and Y directions and corresponding elongated periods. Sa_{S2} stands for the spectral acceleration at the averaged

period, $\overline{T} = (T_x + T_y)/2$, of the structure in the two main building orthogonal directions, X and Y (as proposed for 3D structural models by FEMA P-58, 2012). Its corresponding vector IM is Sa_{V2}, which includes such averages centered at $0.5 \cdot \overline{T}$, $\overline{T}$ and $1.5 \cdot \overline{T}$. Note that, to avoid problems caused by multi-collinearity of different predictors in the regression analyses to come, in the vector IMs of Sa_{V1} and Sa_{V2}, all of the spectral accelerations, other than the first component of the vector, are normalized to the previous component. This artifact significantly reduces the correlation between each vector components.

In addition, Sa_{S3} and Sa_{S4} represent average spectral acceleration (Cordova et al., 2000; Bianchini et al., 2009) in two different formats. Sa_{S3} consists of spectral acceleration at six relevant periods, three for each one of the two main orthogonal horizontal directions of the building: the first mode period, a period longer than the first mode ($\alpha_u \cdot T_1$) and a period shorter than the first mode corresponding to higher modes ($\alpha_1 \cdot T_1$). The quantities α_1 and α_u are defined in Table 1 for each building. Sa_{S4} considers a range of periods (ten for each main orthogonal directions of the building for a total number of twenty) that brackets the first modal period. The corresponding vectors Sa_{V3} and Sa_{V4} have the same components that are averaged in Sa_{S3} and Sa_{S4}. The difference is in the spectral accelerations from X and Y components of the ground motions that are separated in two to form the vector IMs. Finally, PGA as one of the best-known and ubiquitous scalar IMs is also added for comparison purposes. It should be noted that, in all of these cases, except for Sa_{S2}, Sa_{V2} and PGA that use the geometric mean of spectral accelerations extracted from the ground motion horizontal components, the values are based on spectral accelerations from the arbitrary ground motion component. It is stressed here that there is full consistency for all these IMs in the hazard calculation and response estimation. In particular the definition of the sigma in the GMPE considers whether the IM is extracted from an arbitrary component or whether it is calculated using the geometric mean definition (Baker and Cornell, 2006). More information about the criteria that guided the definition of these IMs for response prediction could be found in Kohrangi et al. (2015c).

CASE STUDY BUILDINGS, SITE SPECIFIC PSHA AND RECORD SELECTION

Three examples of 3-, 5- and 8-story buildings representative of typical Southern Europe design and construction practices, designed without provisions for earthquake resistance, are selected for this study (Figure 1). More details about the properties of these building examples, their structural modeling, and their modal, static and dynamic response can be found in Kohrangi et al. (2015c).

A site on the coast of the southern Marmara Sea in Turkey with latitude and longitude of 29.1 and 41.0, respectively, was selected for this study (see Kohrangi, 2015). All sources within 200 km from the site have been considered in the calculations. OpenQuake (Monelli et al., 2012), which is open-source software for seismic hazard and risk assessment developed by the Global Earthquake Model (GEM) organization, was used to perform the seismic hazard computations. These computations are based on the Area Source model and Fault Source and Background (FSBG) model developed during the Seismic Hazard Harmonization in Europe (SHARE) Project (Giardini et al., 2013). The vector PSHA (VPSHA) calculations for all IMs listed in Table 1 were computed via the "indirect" approach to VPSHA (Bazzurro et al., 2009). This method does not use specialized vector PSHA software but rather utilizes the scalar PSHA output results of OpenQuake, that is disaggregation and hazard curves (Kohrangi et al., 2015b).

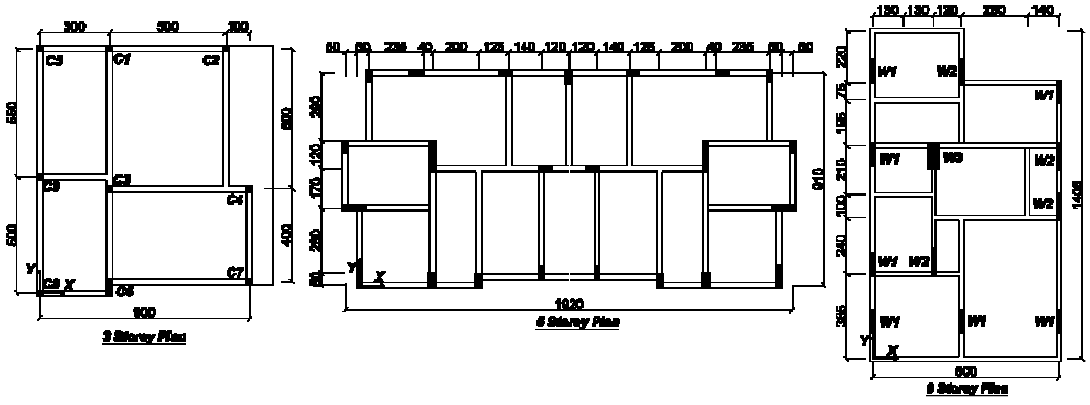

Figure 1**.** Plan view of three tested structural examples (note: dimensions are in cm)

Three sets of records for 10, 12 and 10 IM levels based on the Conditional Spectrum (CS) method (Jayaram et al., 2011) for the periods relevant to the 3-, 5- and 8-story buildings, respectively, were selected. In this methodology, each level of the conditioning IM (which was selected to be Sa_{S2} in this study) uses a suite of 20 two-components ground motion records selected and scaled to match the entire conditional distribution of spectral accelerations, represented by the CS. This way, both the mean and variance of the record set are consistent with the seismic hazard of the site. Kohrangi et al. (2015c) provides the details of record selection and hazard consistency.

RESPONSE AND COLLAPSE ESTIMATION

To gain a continuous representation of the distribution of EDP given IM, a linear regression is utilized of the form $\ln EDP = a + \sum_{i=1}^{n} b_i \cdot \ln IM_i$, where IM_i is the i-th element of the vector IM with n elements, or the single scalar IM and a and b are the regression coefficients (see also Kohrangi et al 2015b). The efficiency (Luco and Cornell, 2007) of each IM presented in Table 1 was compared based on the corresponding conditional dispersion of *EDP|IM* for each building example at each story level and in the two main directions (Kohrangi et al., 2015c). Certainly a suitable IM should be capable of response prediction in terms of structural deflections (e.g., IDR along the height of the building) in the linear and nonlinear ranges of the response since the safety of the building depends on limiting deflections. On the other hand, structural, non-structural and contents in a building are sensitive to different EDPs. Although most of the structural elements are IDR-sensitive, with the notable exception of partitions, non-structural components and contents are mainly PFA-sensitive. However, research has shown that IDR and PFA at different story levels are often best predicted by means of different scalar IMs, which is the opposite of what is done in common practice where $Sa(T_1)$ is applied as the only predictor for all the EDPs everywhere in the building both in the linear elastic and in the severe post-elastic response regimes. As the integration with hazard is much simpler if performed using a single IM as predictor of EDPs, it is a challenge to select one that can improve upon $Sa(T_1)$, that can offer efficient and sufficient response estimation both in the linear elastic and post-elastic range of all required EDPs in the structure, and that is itself predictable (namely has a GMPE developed for it).

Moreover, it is clear that predicting the response of 3D structural models under multi-directional excitation estimated in the main directions of the building requires using separate information from each ground motion component, (Kohrangi et al., 2015c). This fact is particularly significant for asymmetric buildings or for buildings with well separated periods in the two main orthogonal directions. This increased resolution of the response monitoring via multiple direction-specific EDPs is useful for improving damage estimation of building components that are less sensitive to maximum response in the two orthogonal directions or their Square Root Sum of Squares (SRSS) value. In general, it was observed that for an accurate response prediction in terms of IDR in the severe post-elastic range, a more relevant IM that better represents the building response, i.e. a better predictor than $Sa(T_1)$, is required. Such an IM can be the spectral acceleration at an elongated period of the structure (e.g., 1.5 or 2 times T_1, the fundamental period of the structure), that is more related to the nonlinear response of the building (e.g. see Cordova et al., 2000 and Baker and Cornell, 2008). In addition, for tall buildings, influenced by the higher mode effects, spectral accelerations at periods lower than the first modal period are needed within the IM predicting pool. These higher spectral ordinates are also significantly important for PFA estimation especially at the mid-height of the structure.

These observations, at least for the tested buildings, led to the conclusion that an average spectral acceleration in a suitable period range had the potential to provide good response estimation equally appropriate for the PFA and IDR everywhere in the building. An even higher efficiency can be achieved for the response estimation in the X and Y directions when the ground motion excitations were kept separated in a two-component vector (as in Sa_{V3} and Sa_{V4} in Table 1), representing separately the excitation of each direction. This applies especially to 3D asymmetric buildings or to those with well-separated periods in two main orthogonal directions.

As an example of the response analyses results, Figure 2(a) shows the IDR estimates at the first story of the 3-story building and Figure 2(b) displays the building collapse prediction based on logistic regression using the $IM=Sa_{V4}$. Two collapse criteria were considered: the global side-sway collapse, which we equated to the failure in convergence of the Nonlinear

Dynamic Analysis at excessive displacements, and a (largely governing) local collapse criterion corresponding to the exceedance of the median IDR (i.e. 0.04) that can be associated to the loss of load bearing capacity of the non-ductile columns (Aslani, 2005). Following Shome and Cornell (1999), the rate of exceeding different values of an *EDP*, $\lambda(EDP > edp)$, was computed using the conditional complementary cumulative distribution function of *EDP*|*IM* for the non-collapsed data, $\mathrm{P}(EDP > edp \mid \mathrm{NC}, IM)$, and the probability of collapse given *IM*, $\mathrm{P}_{collapse|IM}$, along with the rate of occurrence of the scalar or vector IM of interest, $\lambda(IM)$. Formally:

$$\lambda(EDP > edp) = \int_{IM} \left[\mathrm{P}(EDP > edp \mid \mathrm{NC}, IM) \cdot \left(1 - \mathrm{P}_{collapse|IM}\right) + \mathrm{P}_{\mathrm{collapse}|IM} \right] \cdot \left| d\,\lambda IM \right| \quad (2)$$

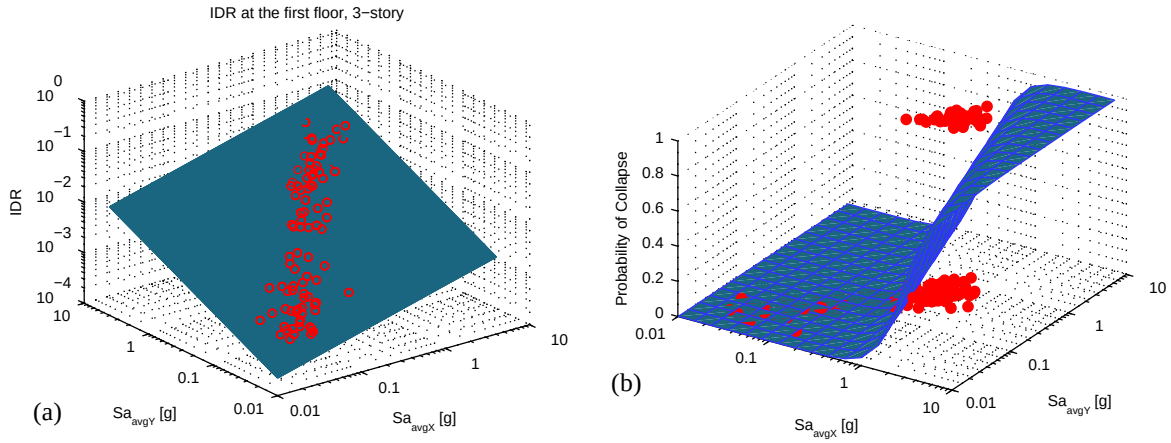

Figure 2. Examples of building response estimation using *IM* = Sa_{V4} as predictor: (a) Response estimation of the SRSS of IDR at the first story for the 3-story building, (b) Collapse fragility surface based on logistic regression (red dots show the binary data: Collapse=1, non-collapse=0).

Logistic regression (Kutner et al., 2005) was used to compute the probability of collapse for each IM level while linear regression was used to model $\mathrm{P}(EDP > edp \mid \mathrm{NC}, IM)$. Figure 3(a) shows the response hazard curve of the MIDR in Y-direction for the 3-story building while Figure 3(b) illustrates the response hazard curve for PFA at the first story of the 3-story

building. The observed scatter in the response of MAR of exceeding low EDP values (i.e., those in the linear or quasi-linear state of the building response) using different IMs is small while it increases for larger EDP values, as expected. Note that since the 3-story building exhibits torsional behavior, the response in one direction is also correlated with the excitation in the orthogonal direction. Thus, IMs that contain information from the excitation in one direction only (such as Sa_{S1}) or the ones that indiscriminately combine the excitations from the two directions (such as Sa_{S2}, Sa_{S3} and Sa_{S4}), introduce more scatter in the response prediction. Therefore, the response hazard curves using such IMs can arguably be considered less reliable.

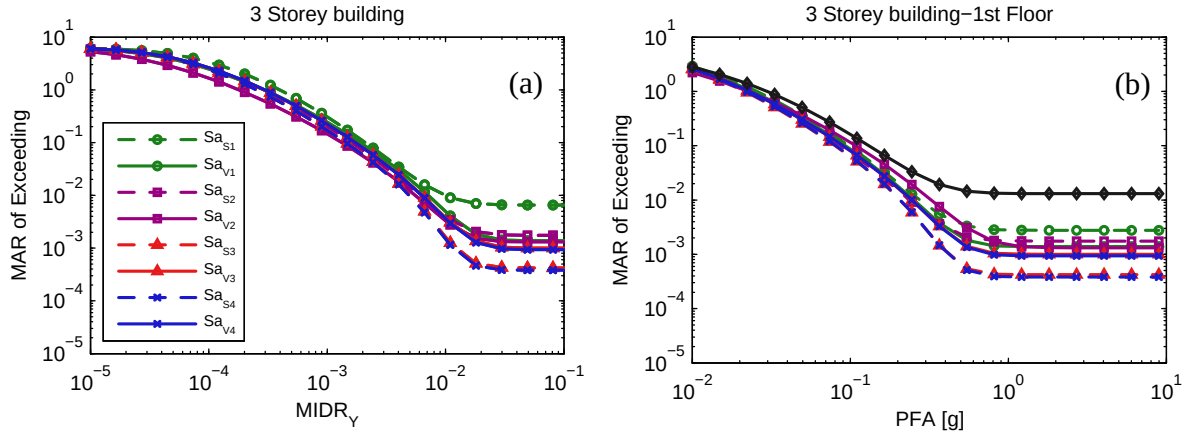

Figure 3. Comparison of response hazard curves obtained using different scalar and vector IM predictors for the 3-story building: (a) Maximum (along the height) Inter Story Drift Ratio in Y direction (MIDRY), (b) PFA at the 1-st floor. The black solid line in the right panel represents PGA.

To engineers the MAR of collapse is the most important estimate to extract from such curves (Zareian and Krawinkler, 2007). To risk analysts the MAR of collapse, which corresponds to losses equal to the replacement cost of the building, are somewhat less crucial since, statistically speaking, these extreme events occur very rarely for engineered buildings. Mathematically, the MAR of collapse, which corresponds to the flat part of a response hazard curve, can be computed as follows:

$$\lambda(collapse) = \int_0^\infty P_{collapse|IM} \cdot \left| d\,\lambda IM \right| \tag{3}$$

Figure 4 presents a summary of the MAR of collapse for the three buildings as estimated using the different IM types considered here and Table 2 summarizes the coefficients of variation of MAR computed a) using the estimates from all the nine IMs (called $C.o.V_{all}$) in Table 1, b) using the estimates only from the four scalar IMs, excluding PGA (called $C.o.V_S$), and c) using the estimates from the four vector IMs (called $C.o.V_V$). As anticipated, the variation in the estimates of MAR from the vector IM cases is much lower than that from the scalar IM cases.

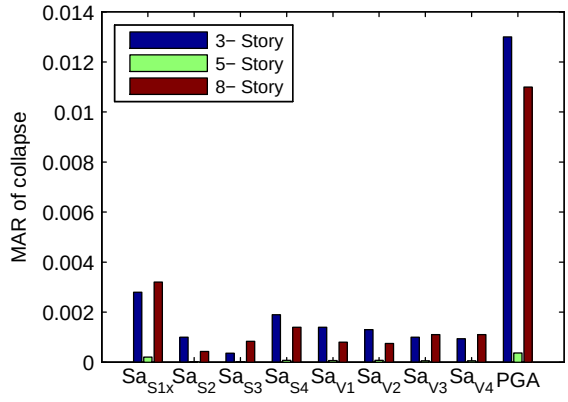

Figure 4. Comparison between MAR of collapse for 3-, 5- and 8-story building and for different scalar and vector IMs.

Table 2. Coefficient of variation of MAR of collapse as estimated using scalar and vector IMs

Building	$C.o.V_{all}$	$C.o.V_S$	$C.o.V_v$
3- story	1.50	0.70	0.19
5- story	1.08	1.09	0.15
8- story	1.47	0.83	0.20

LOSS ESTIMATION

The final target of the applied performance assessment is to estimate the losses in terms of a decision variable. This measure here is defined as the monetary losses, or direct cost of repairing the physical damage suffered by structural and non-structural components of a building. The effect of using different IMs for the EDP prediction is examined based on the building inventory component fragility functions and the corresponding estimated repair or replacement costs. In the following sections, the method used for response and collapse simulation and the building inventory components is explained and finally the results of the analysis for different building examples and different IM types are presented.

RESPONSE SIMULATION METHODOLOGY

The response distribution (parameterized in terms of median and dispersion of EDP|IM) for IDR, PFA, MIDR and MrIDR at each structural level and each direction of the building and the corresponding covariance matrix of all the EDPs were used to simulate the structural demands at each scalar or vector IM level. The response covariance matrix is obtained from the non-collapse data points and, in addition, it is assumed to be constant at all IM levels. The effect of global collapse was incorporated by sampling from the collapse IM distribution obtained from the logistic regression. This assumption of a constant covariance matrix is admittedly an approximation since the correlation between different demand parameters (e.g., IDR at different story levels) does change at different response levels. Note that Jayaram et al. (2012) found that such covariance matrices are relatively constant across different ground motion intensity levels. The effect of this assumption on the results of loss assessment will need to be explored in the future. A more effective approach to resolve the complexity of accounting in terms of EDP correlation matrix would be using IDA or multiple stripe analysis in which the correlation between EDPs is automatically built in each single run. However, these approaches are less practical when we use vector IMs as predictors, as done herein. Hence, we are forced here to work with a cloud of data for response estimation. For this study, the response simulation algorithm proposed by Yang et al. (2006, 2009) for the ATC-58 Project was used. Note that we considered only the record-to-record variability whereas sources of epistemic uncertainty, such as modelling uncertainty, were neglected. The reader interested on the effect of epistemic uncertainty on collapse and loss assessment results is referred to Liel et al. (2009) and Jayaram et al. (2012).

BUILDING INVENTORY FRAGILITY AND CONSEQUENCE FUNCTIONS

The damage state (DS) (i.e., minor damage) that a component of a given subsystem (e.g., columns, beams, walls) at any given story experiences when subject to a certain value of an EDP is simulated based on the fragility function derived here. A component fragility function for a given DS describes the probability of a component reaching or exceeding that DS when subject to various levels of and EDP. Note that the component-based fragility curves are probability-valued functions of the EDP unlike a building fragility function, which is a

probability-valued function of a ground motion IM. The fragility functions utilized to calculate the probability of component *j* (e.g., partitions) at the *k*-th story to be in a damage state ds_i or worse for a given EDP (denoted by EDP_{jk}) are assumed to be cumulative lognormal distribution functions as shown below (Jayaram et al., 2012):

$$\mathrm{P}(DS \geq ds_i \mid EDP_{jk}) = \Phi\left(\frac{\ln(EDP_{jk} / \mu_{ijk})}{\beta_{ijk}}\right), \qquad \textbf{Di}$$

The quantities μ_{ijk} and β_{ijk} denote the corresponding median and dispersion and $\Phi(\cdot)$ is the cumulative distribution function for the standard normal distribution. In this study, for simplicity we considered a perfect correlation between the damage states of components of the same type located at the same floor. In reality, nominally "identical" components may sustain different levels of damage for the same story-specific EDP input as their damage capacity is uncertain and typically not identical. Jalayer and Cornell (2004), Baker (2008) and Bradley and Lee (2010) proposed an approach that considers the dependence in the damage capacity of a component rather than in its damage state.

The fragility and consequence functions of all the components (except infills) were adopted from FEMA P-58 (2012). All the information about these functions as well as the damageable components considered for the three buildings could be found in Kohrangi (2015)-Appendix F. Beam-column joints (used to represent both beam and column damageability as per FEMA P-58), stairs and infill walls are IDR-sensitive. Internal partitions were not included, adopting an open-floor plan that is typical of modern office buildings. For instance, it is assumed that the RC walls aligned with the X direction of the building are only sensitive to the IDRX response of the story where they are located. This assumption may not strictly apply to some structural components that may be sensitive to EDPs in both orthogonal directions in which case a fragility surface rather than a curve may be a more suitable choice. An alternative approach suggested by some researchers is the application of the SRSS of the response (in time) from both orthogonal horizontal directions. For instance, Mitrani-Reiser (2007) showed that this parameter is more useful than others (e.g., maximum IDRX or IDRY or the mean of these two maximum IDRs) for damage estimation of RC columns. As such, following FEMA P-58 (2012), IDRX and IDRY are used to predict losses

for structural walls and their SRSS value (indicated as IDR) is used instead for beam-column joints and concrete stairs.

Most of non-structural elements and contents used here, on the other hand, are PFA-sensitive. It should be noted that the PFA values used herein for all DSs, except for the collapse limit state of the infill walls, are the maximum (in time) SRSS of the PFA values in X and Y directions, since the behavior of these components or contents is assumed to be independent of the direction in which the maximum demand occurs. In any case, we lack the detailed data on how these are oriented in the building at the time of the earthquake to have any chance of a better prediction. In this study, the component fragility function for masonry infill walls is obtained in part based on the experimental data and numerical computations explained in the next section. Finally note that the vertical ground motions were not considered here. The limitation of not having an IM related to the vertical motion at our disposal to use as predictor of EDPs and, in turn, for prediction of damage states may be relevant for some non-structural components, such as suspended ceilings or fire sprinkler piping systems that have been shown to be sensitive to vertical accelerations (see Soroushian et al., 2015 and Ryu et al., 2012, for example).

FRAGILITY FUNCTIONS FOR INFILL WALLS

As mentioned earlier, assuming that the damage of walls occurs mainly in-plane before collapse (Sassun et al., 2016), we selected the value of IDR in the direction of the wall as the EDP, and we defined two Limit States (LS) corresponding to slight and moderate damage. For the collapse LS, however, the damage mechanism is more complex since collapse may happen either in-plane (IP) or out-of-plane (OOP) and the two failure modes are not independent (Kadysiewski and Mosalam, 2009; Morandi et al., 2015). More specifically, Morandi et al. (2015) showed that the OOP strength of the wall reduces as the IP damage increases. Therefore, it is more realistic to consider a collapse fragility surface based on EDPs aligned with the wall direction and with the direction orthogonal to it.

Kadysiewski and Mosalam (2009) derived a model for masonry infill walls together with the collapse criterion that is a function of the IP relative displacement of the infill wall (Δ_{IP})

and the OOP displacement of the wall at mid-height (Δ_{OOP}). This model was also used here in the analytical simulation (in OpenSees, McKenna et al., 2000) of infills for response estimation when nonlinear dynamic analysis is performed. Although these two parameters are physically valid for collapse definition of the wall, alternatively, in a transient analysis, it is intuitive that what triggers the OOP displacement at mid-height of the wall is the floor acceleration (e.g., see Doherty et al. (2002), where the OOP wall model is based on the acceleration of its support). Hence, we defined a collapse fragility surface that is based on IDR in the IP direction and PFA in the OOP direction using the analytical model of Kadysiewski and Mosalam (2009) with the typical properties of the infill walls in the tested buildings. Thus, in our response data obtained from Nonlinear Dynamic Analysis, an approximate equation that defines PFA_{OOP} as a function of Δ_{OOP} was obtained and substituted by Δ_{OOP} in the collapse criterion. Δ_{IP}, on the other hand, was simply normalized by the story height to become the in-plane IDR.

The final collapse criterion is shown in Figure 5(a) and the proposed fragility surface (depicted as discrete lines) is shown in Figure 5(b). Each line in this figure is defined based on the median in-plane IDR (which itself is a function of the PFA_{OOP} demand of every single realization) and the corresponding dispersion. The dispersion values were adopted based on the suggestions of the FEMA P-58 (2012) for analytically derived low-data fragility functions. This fragility surface is approximate and it certainly could be improved by more data and experimental results.

Moreover, we assumed that at a given state of the infill wall during the dynamic analysis, the history of the response does not have any effect on the wall capacity. However, Barrera (2015) showed that, as far as the wall demand level exceeds a certain value, any subsequent damage that occurs to the wall either IP or OOP will accumulate. Therefore, a more accurate model would be the one which keeps the memory of damages within a time history analysis. Due to the complexity of such an approach, in this study we adopted the aforementioned simpler methodology. Despite its limitations, this damage model for infill walls is appropriate for illustrating the applicability of vector IMs as input to EDP and loss estimation, which is one of the purposes of the current study.

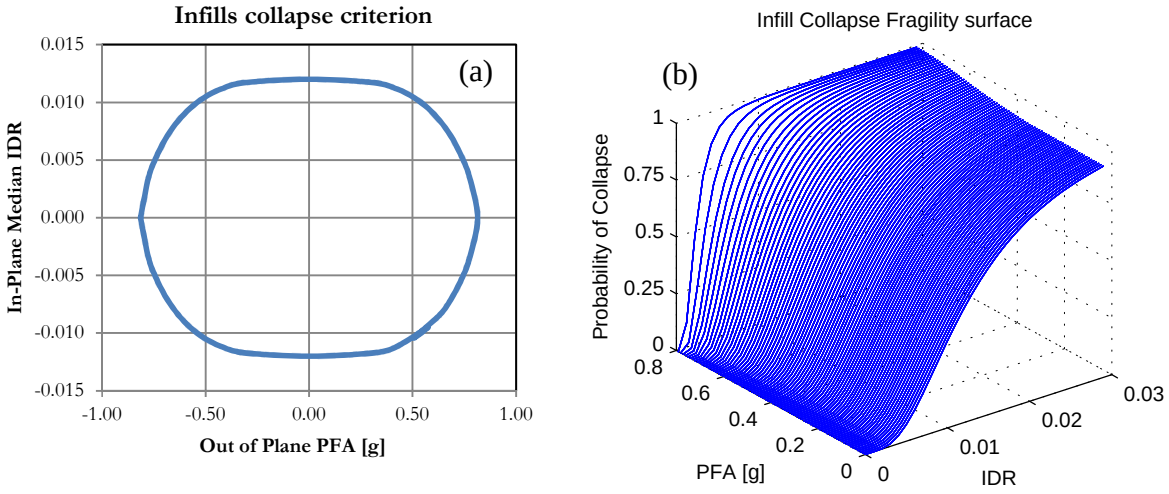

Figure 5. a) Infill walls collapse criterion surface; b) Infill walls collapse fragility surface

LOSS RESULTS AND DISCUSSION

We computed the monetary loss distributions for different IMs and building models Based on the aforementioned framework. The resulting estimates of the median and dispersion of the losses for the 5-story building predicted using the six scalar IMs in Table 1 are shown Figure 6. Figure 6(a) shows the median loss for the entire building normalized by its replacement cost ratio as a function of the return period of the IM used as predictor of the EDP. These figures suggest that the median loss estimates computed by different ensembles of records conditioned on different IMs having the same return period at the site are not unique. The different estimates of the median loss depend on the predictability of the IM (i.e., the dispersion of the given ground motion rupture $\sigma_{IM|rup}$ from the GMPE), on the efficiency of the IM in predicting the EDP of choice (i.e., $\sigma_{EDP|IM}$), and on the uncertainty in the component repair cost for a given damage state (Aslani, 2005; Goulet et al., 2007; Bradley et al., 2009b). Since the uncertainty in the repair cost for a given damage state of the component is independent of the IM choice in the loss computations and the same set of records was used in the nonlinear response history analysis (implicitly assuming that hazard consistency is assured regardless of the IM used for integration, see Kohrangi et al. 2015c), the difference in the loss distributions can only be explained by the difference in predictability and efficiency of each IM. It was shown in Kohrangi et al. (2015c) that, in

general, the average spectral acceleration (Sa_{S3} and Sa_{S4}) tends to decrease the dispersion in estimating both IDR and PFA along the height of the building compared with the more common cases of Sa_{S1} and Sa_{S2}. In addition, it was shown in Kohrangi et al. (2015a) that the averaged spectral acceleration has a significantly higher predictability (i.e. lower $\sigma_{IM|rup}$) than the spectral acceleration at any given period. Therefore, the higher efficiency and predictability of average spectral accelerations Sa_{S3} and Sa_{S4} may be the reason for the lower median loss estimates (Figure 4a) obtained when using Sa_{S3} and Sa_{S4}.

The logarithmic standard deviation of the loss given intensity (at equivalent return periods from seismic hazard) for the 5-story building is shown in Figure 6(b). While the median loss increases with the severity of the IM level, the dispersion of the loss estimates reduces as the loss distribution converges to the building replacement cost, as also observed by Krawinkler (2005) and Bradley et al. (2009a). Visual illustration of the median loss values for vector IM cases with more than two components is, of course, not possible. The median loss ratios based on the two-component vector of Sa_{v4} for the 3-story building is shown in Figure 7(a). Figure 7(b) depicts instead the variation of the probability of collapse of the 8-story building with the return period of the IM levels as computed for the six different scalar IMs in Table 1. Again the estimates of the collapse probabilities determined using the vectors Sa_{S3} and Sa_{S4} are significantly lower than those derived form the use of less efficient and predictable IMs.

To gain additional insights about the differences in loss estimation caused by the choice of IM and on the components that contribute to losses at different levels of ground shaking, Figure 8 compares the breakdown of losses by component class for the 5-story building obtained using the ground motion records conditioned on the scalar IMs of Sa_{S1x} and Sa_{S4} corresponding to the 50% and 10% in 50 years events. The efficiency of the IM has a crucial role in predicting the distribution of the losses at any intensity level. By inspecting Figure 8(a) and Figure 8(c) it is clear that most of the loss contributions at 50% in 50 years event come from the infill walls and the acceleration-sensitive components. The analyses conditioned on Sa_{S4}, however, predict smaller loss percentage for beam column joints than those based on Sa_{S1x}. At higher intensity levels such as 10% in 50 years (Figure 8b and Figure

8d), the contribution of displacement-sensitive components becomes more significant. The fraction of losses due to collapse and demolition are not significant loss factors for the 50% in 50 years probability of exceedance levels shown here. Of course, their contribution to the total losses generally grows with the intensity of the ground motions.

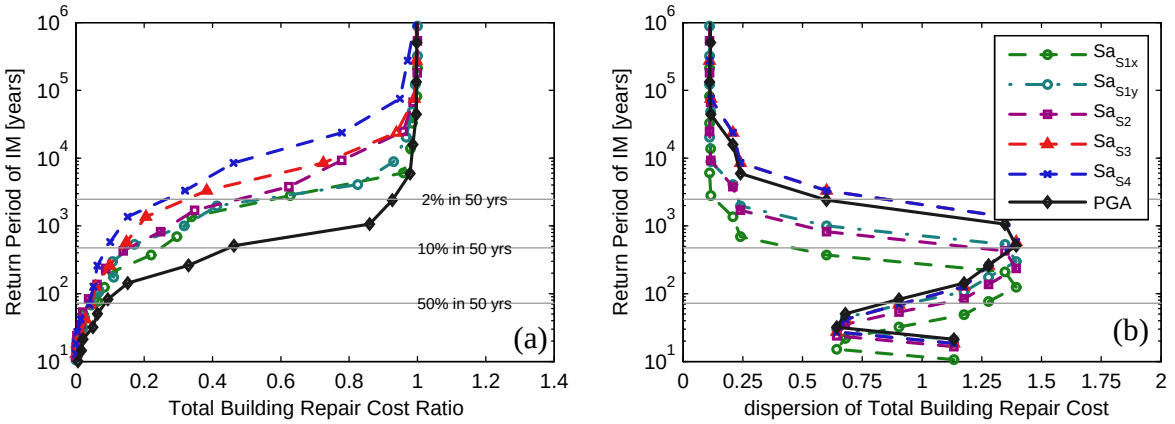

Figure 6. Parameters of distributions of losses normalized by the building replacement cost for the 5-story building computed using scalar IMs: (a) median, (b) dispersion.

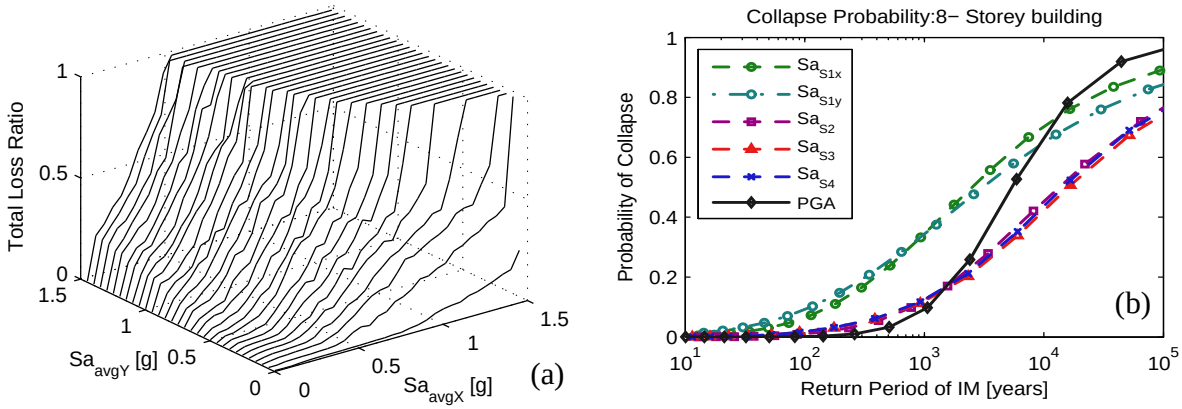

Figure 7. (a) Median loss values when using vector IM of Sa_{V4} for the 3-story building. (b) Probability of collapse for the 8-story building given different scalar IMs.

As can be seen in Figure 8(b) and Figure 8(d), the choice of IM leads to quite different damage predictions for the same intensity return period of 10% in 50 years. Sa_{S1x} predicts that the building is more vulnerable. In fact there is around 30% probability of replacing the building. Sa_{S4}, on the other hand, predicts a lower total cost with damages mostly confined to

the nonstructural elements and negligible probability of collapse or demolition. Two engineers, therefore, performing the same analysis but using two different IMs may draw quite different conclusions on the safety and losses of the building. We claim here that, perhaps the IM with higher sufficiency and efficiency may provide the better estimate.

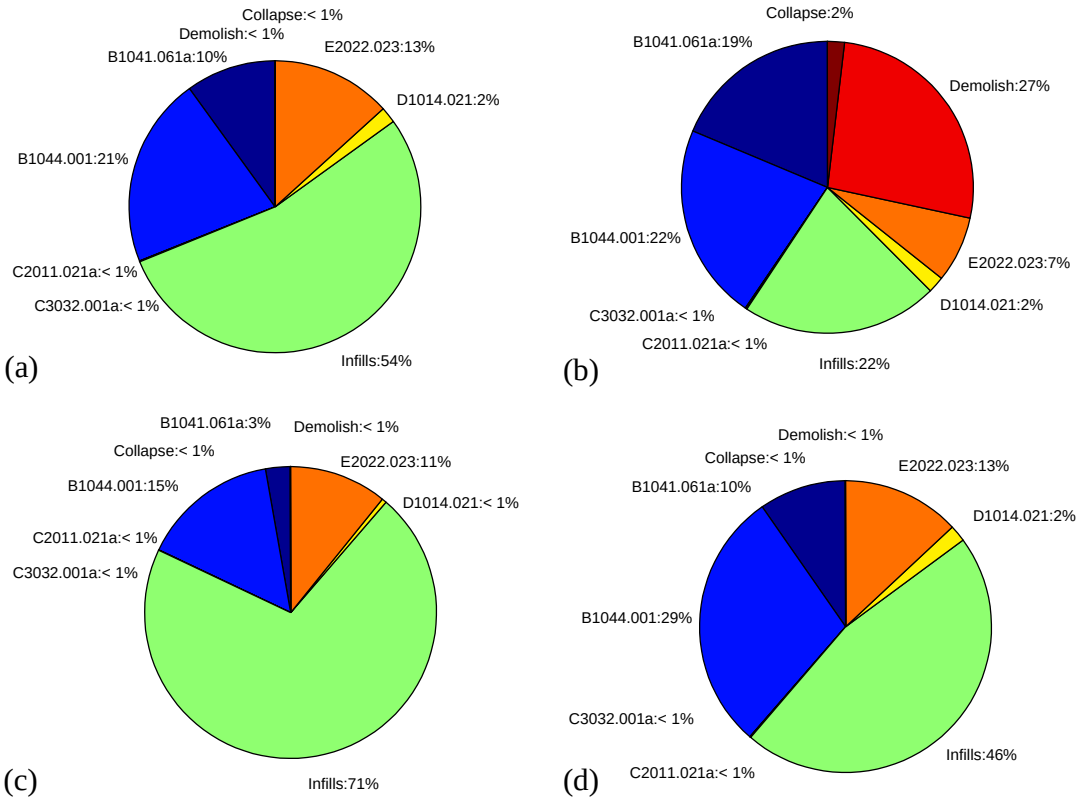

Figure 8. Disaggregation of Losses for of the 5-story building conditioned on (a) Sa_{S1x} at the 50% in 50 years probability of exceedance (PE), (b) Sa_{S1x} at the 10% in 50 years PE, (c) Sa_{S4} at the 50% in 50 years PE, (d) Sa_{S4} at the 10% in 50 years PE. Legend: B1041.061a: Beam-column joints; B1044.001: Rectangular RC walls C2011.021a: Concrete stairs; C3032.001a: suspended ceilings; D1014.021: Hydraulic Elevator; E2022.023: Desktop Electronics.

Why records conditioned on different IMs having the same PE in 50 years at the site predict different losses and different loss breakdowns? It was pointed out in Kohrangi et al. (2015c) that the effectiveness of average spectral acceleration, such as Sa_{S4}, in predicting different EDP types is a function of the weights (i.e. the number) of the spectral ordinates at periods lower and higher than the fundamental period T_1 of the structure. Having more

ordinates at periods shorter than T_1 gives more weight to higher modes, improving PFA prediction. Having more ordinates at periods longer than T_1 improves the estimation capability for displacement-sensitive components and global collapse. In this case SaS4 has a higher weight at the low period ranges and, therefore, it is a better IM for prediction of PFAs while it tends to under-predict the EDP for the displacement-sensitive components, namely IDR here. In other words, different definitions of the average spectral acceleration represent different compromises in accuracy between PFA and IDR prediction. The vector IMs, by virtue of separation of ordinates, can be made less sensitive to this effect.

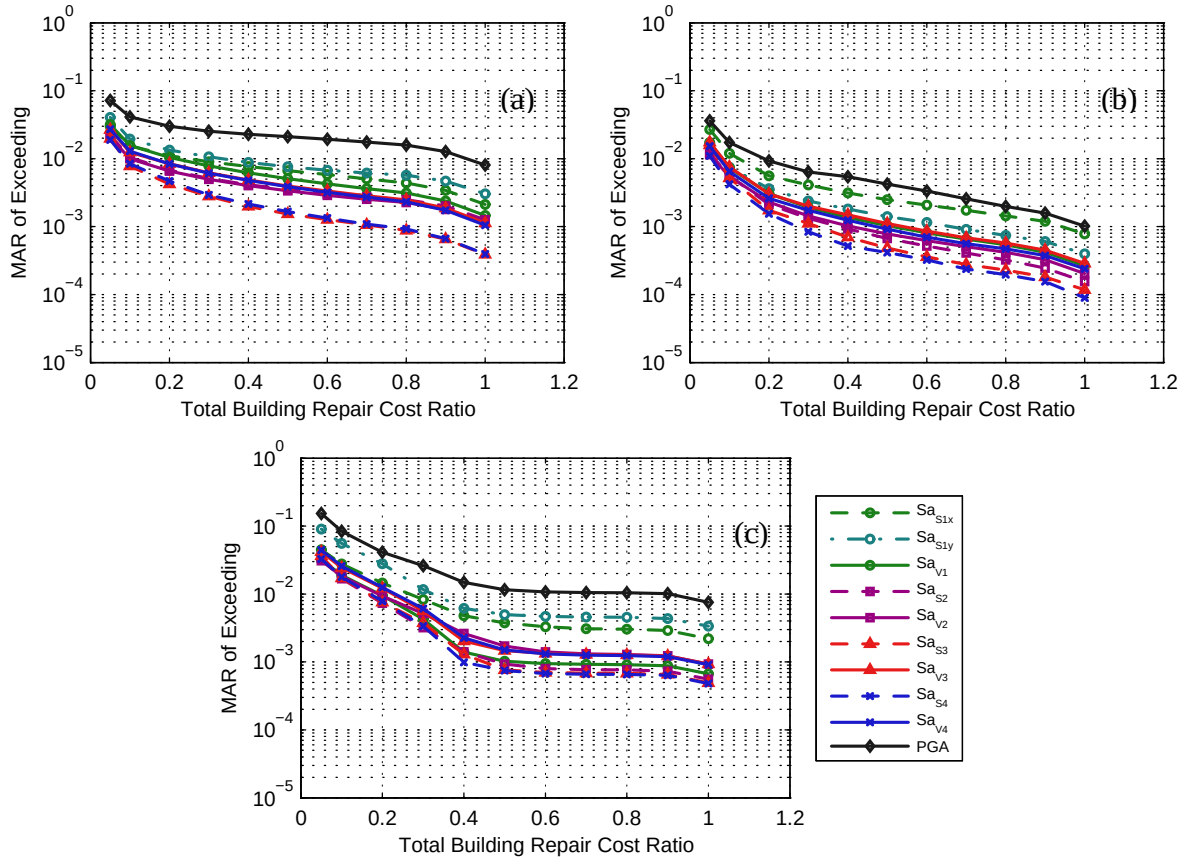

Figure 9. MAR of exceeding the total building loss ratio: a) 3-story, b) 5-story and c) 8-story buildings

The values of the MAR of exceeding the building loss ratios as estimated using different IMs (scalar and vector) for the three building examples are shown in Figure 9. There is a common trend in all of the figures: PGA followed by Sa_{S1x} and Sa_{S1y} , namely the three scalar

IMs, provide the highest exceeding rates and the Sa_{S3} and Sa_{S4}, namely two average spectral acceleration IMs, provide the lowest. It is interesting to note also that the vector IM cases have the lowest scatter and, therefore, we can argue that by use of vector IMs the estimates of the loss MAR get closer to the "true" but unknown answer. We do not have solid evidence on what the "true" response is, as we do not have a "perfect" reference value to compare against. It is, however, likely that the MAR of losses that are estimated using the scalar IMs Sa_{S1x} and Sa_{S1y} are farther from the "true" answer and quite likely biased high. The consistency in the MAR values provided by the vector results points towards a higher fidelity, potentially indicating that they are closer (in the 3D examples tested) to providing an accurate answer.

Another useful metric in loss assessment is the Expected Annual Loss (EAL), which is the long-term average annual economic loss that the building is expected to experience due to earthquakes at that site. The EAL is useful to many stakeholders as the basis to make informed decisions about risk mitigation. An owner may use it for example to decide whether buying earthquake insurance and/or retrofitting the building, while an insurance company uses it to set the technical premium that supports the computations of the insurance premiums offered to potential customers (Aslani, 2005). An estimate of the EAL can be computed as:

$$EAL = \int_0^\infty c \cdot \left| d\lambda_c \right| \tag{5}$$

In which λ_c is the MAR of exceeding the cost value of c. If c is defined as a cost ratio instead, then the EAL ratio is provided by Equation (5). The EAL ratios obtained conditioning on different IMs are compared in Figure 10. The differences in the EAL estimates from the vector cases and from the cases that use simple IMs, such as Sa_{S1x}, Sa_{S1y} and PGA are very significant. On the other hand, the differences between the MAR estimates from vector IM cases and scalar IM cases based on averaged spectral accelerations are somewhat less relevant. Note that this figure also shows the difference in the estimates of the EAL ratios that stems from the consideration for infill walls of the out-of-plane failure mode in addition to the in-plane one. The cases with and without interaction in the infill wall failure modes are only slightly different. This small difference, however, cannot be generalized, and may be due to the simplified failure model implemented here.

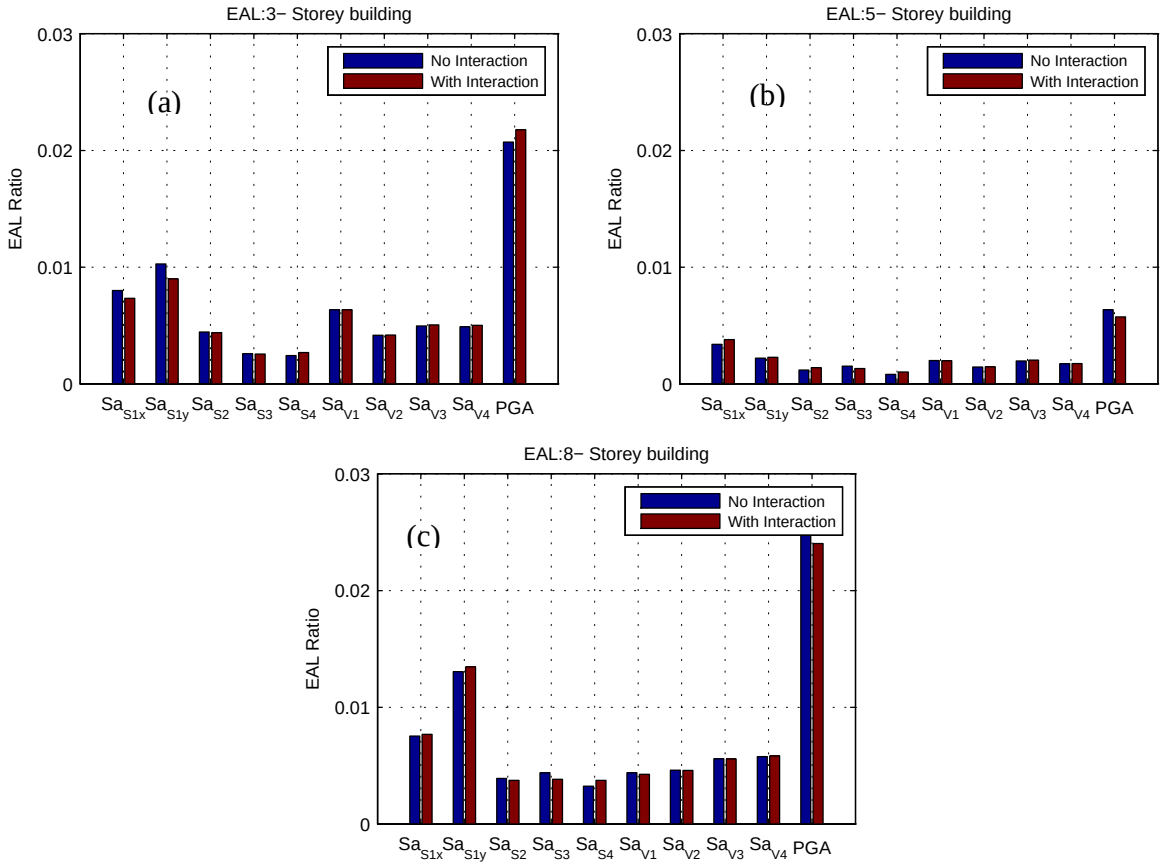

Figure 10. Expected Annual Loss ratio: comparison between estimates obtained from different IM types using infill collapse fragility curves with/without interaction: a) 3-story; b) 5-story and c) 8-story.

CONCLUSIONS

The main focus of this study is to extend the current state-of-the-art PBEE procedure based on PEER Center style for building-specific loss estimation beyond the use of simple ground motion Intensity Measures (IMs) as predictor of Engineering Demand Parameters (EDPs) and, in turn, of damage states and losses for realistic 3D structural models. This approach allows detailed component-based loss analysis considering the vector of building EDPs locally at all stories rather than using only one global response parameter (e.g., the maximum inter story drift ratio). The investigated set of IMs still considers simple scalar spectral acceleration and PGA, as reference to common practice. However, it also includes average spectral acceleration in a period range relevant to the specific building under

consideration and also various combinations of vector IMs that preserve the direction of action of the ground motion. The ground motion IM used as input to the response of these buildings is kept fully consistent with the hazard, which has been probabilistically computed for the same IM, be it simple or complex, scalar or vector, using appropriate Ground Motion Prediction Equations. Three 3D building examples of 3-, 5- and 8-story RC infilled frames, typical of old Mediterranean construction were considered as test cases for testing this methodology.

A procedure for considering the effect of the infill walls in-plane and out-of-plane interaction based on a function of the infill demand was also implemented. However, for the building examples tested here and compared with the total building repair cost, insignificant changes were observed in the total loss values and the Expected Annual Loss. Based on the methodology introduced in this study, this approach could be adopted for other types of building components (e.g., suspended ceilings) that are sensitive to more than one EDP.

To conclude, it should be noted that all the IMs utilized in this study represent legitimate choices that are usable in practice. However, the results presented show that there is significant scatter in the estimates of the MAR of exceedance of losses. This large difference may pose a question mark about the effectiveness of such simple scalar IMs in capturing well the story-specific engineering demand parameters needed for assessing losses in 3D structural models. The spectral acceleration at the first mode of vibration of the structure (Sa_{s1x} and Sa_{S1y}) and PGA, provide loss estimates that can arguably be considered as conservative when compared to those of the other sophisticated scalar and vector IMs tested here. When vector IMs are used, at least of the kind utilized here, the scatter in loss estimates is considerably tightened and the bias may be at least partially removed. The use of vector IMs both in hazard assessment and response estimation, might be considered cumbersome and less appealing in practice. However, using a vector IM, at the very least, can provide important insights on how far from the ‘true’ yet unknown response the MAR estimates obtained via simpler scalar choices lie. Although only three buildings were studied and more research is still needed, it can be claimed that the loss assessment of 3D structures can benefit considerably from the explicit consideration of seismic intensity in the two orthogonal

directions, preferably in a vector form or, at least, in a sophisticated scalar form, such as those based on spectral acceleration averaged over a building-specific period range.

ACKNOWLEDGMENTS

We would like to thank Dr. Marco Pagani for his precious help on carrying out the PSHA analysis for this study. The support from Dr. Jaesung Park for generating the VPSHA code developed for this study is also very much appreciated. We hereby acknowledge that the building data used was in part provided by Prof. Fabrizio Mollaioli, Prof. Rui Pinho and Dr. Romain Sousa. Partial support was provided to the second author by the European Research Executive Agency via Marie Curie grant PCIG09-GA-2011-293855.

REFERENCES

Aslani, H., and Miranda, E., 2005. Probabilistic earthquake loss estimation and loss disaggregation in buildings. *Ph.D. thesis*, John A. Blume Earthquake Engineering Centre, Department of Civil and Environmental Engineering, Stanford University.

Baker J.W. and Cornell, C. A., 2006. Which Spectral Acceleration Are You Using? . *Earthquake Spectra*. **22** (2):293–312.

———, 2008. Vector-valued intensity measures incorporating spectral shape for prediction of structural response. *Journal of Earthquake Engineering*. **12** (4):534–554.

Baker, J. W., 2007. Probabilistic structural response assessment using vector-valued intensity measures. *Earthquake engineering and structural dynamics*. **36** (13):1861–1883.

———. 2008. Introducing correlation among fragility functions for multiple components. *Proceedings, 14th World Conference on Earthquake Engineering, Beijing, China*.

Barrera, M. J., 2015. Masonry Infill Wall Collapse Fragilities. *M.Sc. thesis*, UME School/ROSE Pragramme, IUSS Pavia.

Bazzurro, P., Tothong, P., Park, J. 2009. Efficient Approach to Vector-valued Probabilistic Seismic Hazard Analysis of Multiple Correlated Ground Motion Parameters. *Proceedings, 10th International Conference on Structural Safety and Reliability (ICOSSAR09), Osaka, Japan*.

Bianchini, M., Diotallevi, P., and Baker, J. W. 2009. Prediction of Inelastic Structural Response Using an Average of Spectral Accelerations. *Proceedings, 10th International Conference on Structural Safety and Reliability (ICOSSAR09), Osaka, Japan*.

Bradley, B. A., and Lee, D.S., 2010. Component correlations in structure-specific seismic loss estimation. *Earthquake engineering and structural dynamics*. **39** (3):237–258.

Bradley, B. A., Dhakal R.P., MacRae, G.A., and Cubrinovski, M., 2009a. Prediction of spatially distributed seismic demands in specific structures: Ground motion and structural response. *Earthquake engineering and structural dynamics*. **39**:501–520.

———, 2009b. Prediction of spatially distributed seismic demands in specific structures: Structural response to loss estimation. *Earthquake engineering and structural dynamics*. **39**:591–613.

Cordova, P. P., Deierlein, G.G., Mehanny, S.S., and Cornell, C.A. 2000. Development of a two-parameter seismic intensity measure and probabilistic assessment procedure. *Proceedings, 2nd US–Japan Workshop on Performance-based Earthquake Engineering Methodology for RC Building Structures, Sapporo, Hokkaido, 2000.*

Doherty, K., Griffith, M.C., Lam, N., and Wilson, J. , 2002. Displacement-based seismic analysis for out-of-plane bending of unreinforced masonry walls. *Earthquake engineering and structural dynamics*. **31** (4):833–850.

Faggella, M., Barbosa, A.R., Conte, J.P., Spacone, E., and Restrepo, J.I. , 2013. Probabilistic seismic response analysis of a 3-D reinforced concrete building. *Structural Safety*. **44**:11–27.

FEMA, 2012. Seismic Performance Assessment of Buildings, FEMA P-58-1. *Applied Technology Council for the Federal Emergency Management Agency*.

Giardini, D., et al., 2013. Seismic Hazard Harmonization in Europe (SHARE). *Online data resource, Swiss Seismological Service*.ETH Zurich, Zurich, Switzerland, [Available at: http://www.efehr.org:8080/jetspeed/].

Goulet, C. A., Haselton, C.B., Mitrani-Reiser, J., Beck, J.L., Deierlein, G.G., Porter, K., and Stewart, J.P., 2007. Evaluation of the seismic performance of a code-conforming reinforced-concrete frame building—from seismic hazard to collapse safety and economic losses. *Earthquake engineering and structural dynamics*. **36** (13):1973–1997.

Jalayer, F., and Cornell, C.A., 2004. *A technical framework for probability-based demand and capacity factor design (DCFD) seismic formats*. PEER Report 2003/08, Pacific Earthquake Engineering Research Center, University of California, Berkeley.

———, 2009. Alternative nonlinear demand estimation methods for probability-based seismic assessments. *Earthquake engineering and structural dynamics*. **38** (8):951–972.

Jayaram, N., Lin, T., Baker, J.W., 2011. A Computationally Efficient Ground-Motion Selection Algorithm for Matching a Target Response Spectrum Mean and Variance. *Earthquake Spectra*. **27** (3):797–815.

Jayaram, N., Shome, N., Rahnama, M., 2012. Development of earthquake vunerability functions for tall buildings. *Earthquake Engineering & Structural Dynamics*. **41**:1495–1514.

Kadysiewski, S., and Mosalam, K.M., 2009. *Modeling of Unreinforced Masonry Infill Walls Considering In-plane and Out-of-Plane Interaction*. PEER Report 2008/102, Pacific Earthquake Engineering Research Center, University of California, Berkeley.

Kazantzi, A. K., and Vamvatsikos, D., 2015. Intensity measure selection for vulnerability studies of building classes. *Earthquake engineering and structural dynamics*. DOI: 10.1002/eqe.2603.

Kennedy, R. P., and Ravindra, M.K., 1984. Seismic fragilities for nuclear power plant risk studies. *Engineering and Design*. **79** (1):47–68.

Kohrangi, M., 2015. Beyond scalar Intensity Measures in seismic risk assessment. *PhD Thesis*, UME School/ROSE Programme, IUSS-Pavia.

Kohrangi, M., Bazzurro, P., and Vamvatsikos, D., Spillatura, A., 2015a. Conditional Spectrum-based ground motion selectuon using average spectral acceleration. *Earthquake engineering and structural dynamics*. *(Under review).*

———, 2015b. Vector and Scalar IMs in Structural Response Estimation: Part I–Hazard Analysis. *Earthquake Spectra (Accepted)*.

———, 2015c. Vector and Scalar IMs in Structural Response Estimation: Part II–Building Demand Assessment. *Earthquake Spectra. (Accepted)*.

Krawinkler, H., 2005. *Van Nuys hotel building testbed report: exercising seismic performance assessment*. PEER Report 2005/11, Pacific Earthquake Engineering Research Centre, University of California, Berkeley.

Kutner, M. H., Nachtsheim, C.J., and Neter, J., 2005. *Applied linear regression models (5-th edition)*, McGraw-Hill/Irwin: New York.

Liel, A. B., Haselton, C.B., Deierlein, G.G., and Baker, J.W., 2009. Incorporating modeling uncertainties in the assessment of seismic collapse risk of buildings. *Structural Safety*. **31** (2):197–211.

Lucchini, A., Mollaioli, F., and Monti, G., 2011. Intensity measures for response prediction of a torsional building subjected to bi-directional earthquake ground motion. *Bulletin of Earthquake Engineering*. **9** (5):1499–1518.

Luco, N., 2002. Probabilistic seismic demand analysis, SMRF connection fractures, and near-source effects. *Ph.D. thesis*, Dept. of Civil and Env. Engineering, Stanford University, California.

Luco, N., and Cornell, C.A., 2007. Structure-Specific Scalar Intensity Measures for Near-Source and Ordinary Earthquake Ground Motions. *Earthquake Spectra*. **23** (2):357–392.

McKenna, F., Fenves, G., Jeremic, B., and Scott, M. 2000. Open system for earthquake engineering simulation. <http://opensees.berkeley.edu> (Jan 2014).

Mitrani-Reiser, J., 2007. An ounce of prediction: probabilistic loss estimation for performance-based earthquake engineering. *Ph.D. thesis*, California Institute of Technology, Pasadena, California.

Modica, A., and Stafford, P.J., 2014. Vector fragility surfaces for reinforced concrete frames in Europe. *Bulletin of Earthquake Engineering,*. **12**:1725–1753.

Monelli, D., Pagani, M., Weatherill, G., Silva, V., and Crowley, H. 2012. The hazard component of OpenQuake: The calculation engine of the Global Earthquake Model. *Proceedings, 15th World Conference on Earthquake Engineering, Lisbon, Portugal*.

Morandi, P., Hak, S., and Magenes, G. 2015. Simplified Out-of-plane Resistance Verification for Slender Clay Masonry Infills in RC Frames. Dipartimento di Ingegneria Civile ed Architettura: Università degli Studi di Pavia ed EUCENTRE.

Mosalam, K. M., and Günay, S. 2015. Progressive Collapse Analysis of Reinforced Concrete Frames with Unreinforced Masonry Infill Walls Considering In-Plane/Out-of-Plane Interaction. *Earthquake Spectra*, **31**(2), 921–943.

Porter, K. A., Beck, J.L., and Shaikhutdinov, R., 2002. Sensitivity of Building Loss Estimates to Major Uncertain Variables. *Earthquake Spectra*. **18** (4):719–743.

Porter, K. A., Kennedy R.P., and Bachman R.E., 2007. Creating fragility functions for performance-based earthquake engineering. *Earthquake Spectra*. **23** (2):471–489.

Porter, K. A., Kiremidjian, A.S., and LeGrue, J.S., 2001. Assembly-Based Vulnerability of Buildings and its Use in Performance Evaluation. *Earthquake Spectra*. **17** (2):290–312.

Ramirez, C. M., and Miranda, E., 2009. Building specific loss estimation methods and tools for simplified performance-based earthquake engineering. *Ph.D. thesis*, John A. Blume Earthquake Engineering Centre, Department of Civil and Environmental Engineering, Stanford University.

Ryu, K. P., Reinhorn, A.M. and Filiatrault, A. 2012. Full Scale Dynamic Testing of Large Area Suspended Ceiling System. *Proceedings, 15th World Conference on Earthquake Engineering, Lisbon, Portugal*.

Sassun, K., Sullivan, T.J., Morandi, P., Cardone, D., 2016. Characterising the in-plane seismic performance of infill masonry. *Bulletin of the New Zealand Society for Earthquake Engineering (under review)*.

Shome, N., Cornell, C.A., 1999. Probabilistic seismic demand analysis of nonlinear structures. *Report No. RMS-35.*, John A. Blume Earthquake Engineering Centre, Department of Civil and Environmental Engineering Stanford University.

Soroushian, S., Zaghi, A., Maragakis, M., Echevarria, A., Tian, Y., and Filiatrault, A., 2015. Analytical Seismic Fragility Analyses of Fire Sprinkler Piping Systems with Threaded Joints. *Earthquake Spectra*. **31** (2):1125–1155.

Vamvatsikos, D., and Cornell C.A., 2002. Incremental dynamic analysis. *Earthquake Engng. Struct. Dyn.* **31** (3):491–514.

Yang, T. Y., Moehle, J., Stojadinovic, B., and Der Kiureghian, A. 2006. An application of PEER performance-based earthquake engineering methodology. *Proceedings, 8th U.S. National Conference on Earthquake Engineering, San Francisco, California*.

———, 2009. Seismic performance evaluation of facilities: methodology and implementation. *Journal of Structural Engineering*. **135** (10):1146–1154.

Zareian, F., and Krawinkler, H., 2007. Assessment of probability of collapse and design for collapse safety. *Earthquake engineering and structural dynamics*. **36** (13):1901–1914.